Forschungszentrum Karlsruhe
in der Helmholtz-Gemeinschaft
Institut für Materialforschung II

RICAM, Linz — October, 6th– 7th, 2005
Miniworkshop "Direct and Inverse Problems in Piezoelectricity"

Constitutive Properties of Ferroelectric Piezoceramics: Experimental Investigation, Microscopically Motivated Modeling, Finite Element Simulation

Marc Kamlah, Dayu Zhou, Bernd Laskewitz, Zhenggui Wang

- ferroelectric piezoceramics
- response behavior under large signal electro-mechanical loading
- micromechanical polycrystalline volume element
- micromechanically motivated constitutive model
- finite element simulation of poling processes

piezoceramics

ferroelectric ceramics

- $BaTiO_3$, $Pb(Zr_xTi_{1-x})O_3$ mixed oxid: PZT
- paraelectric-ferroelectric phase transition

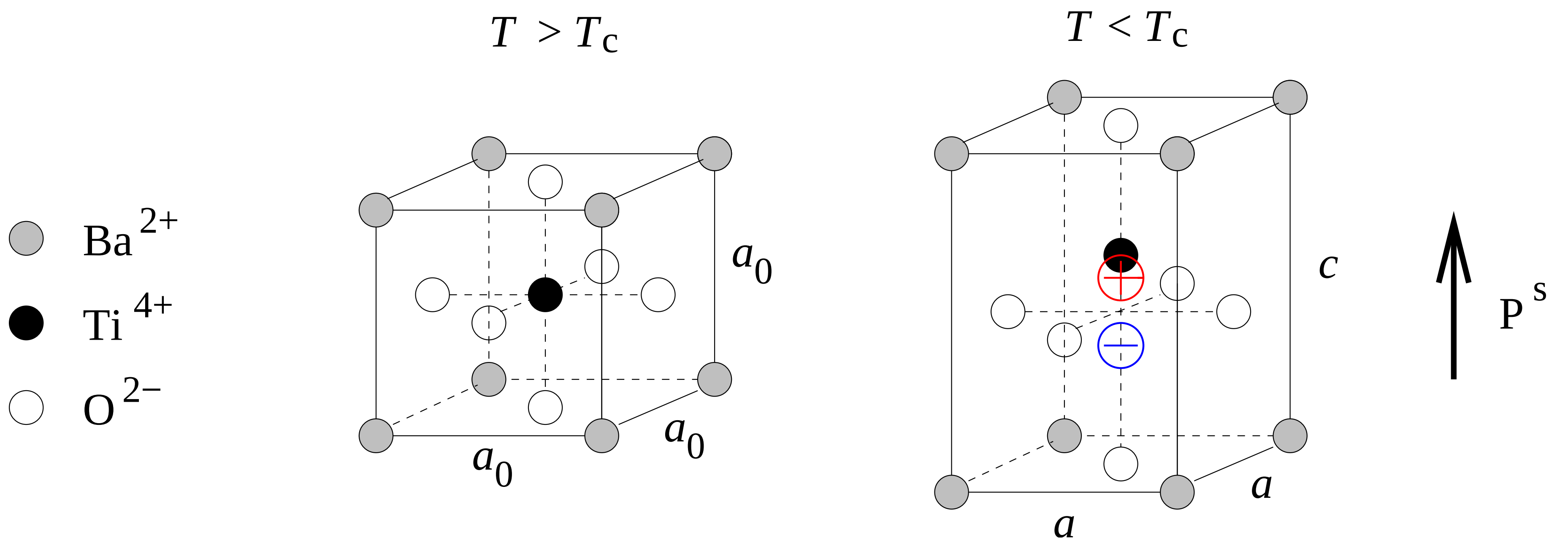

$$\frac{c - a_0}{a_0} \approx 0.5...1.0\%$$

$\longrightarrow$ spontaneous polarization and spontaneous strain

$\longrightarrow$ direct und inverse piezoelectric effect (unit cell)

piezoceramics

- 6 variants at phase transition

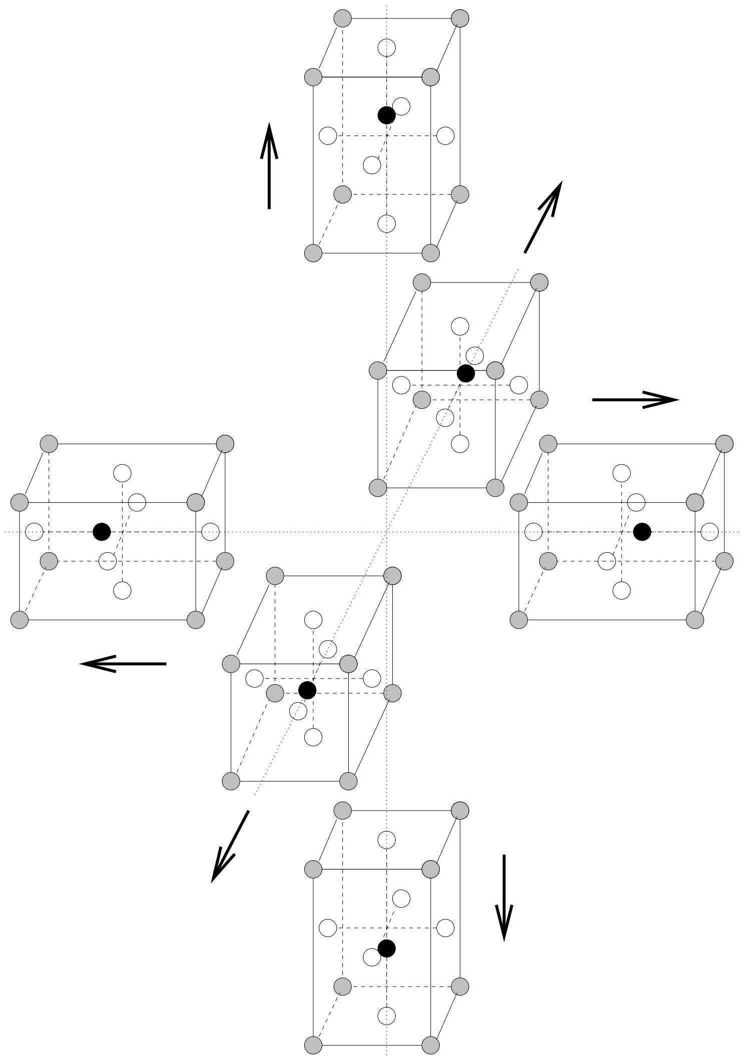

- occurence of domains

  as substructure in each grain

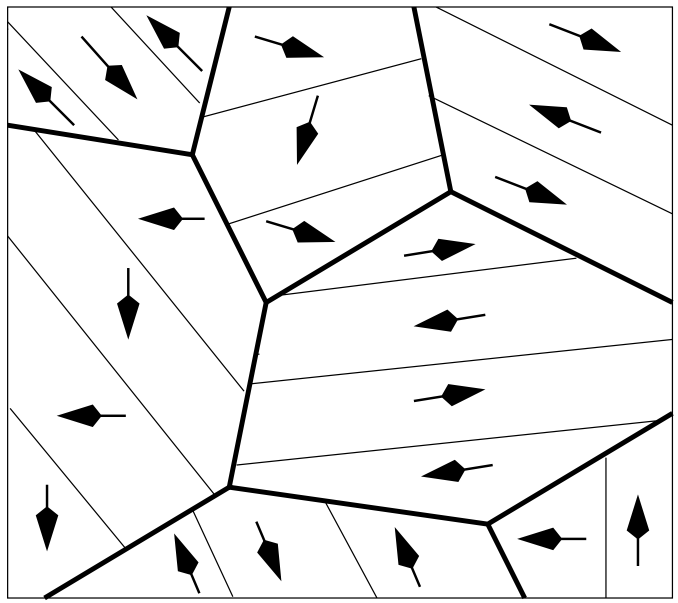

$\longrightarrow$ macroscopic isotropy

after sintering

piezoceramics

- polycrystalline $BaTiO_3$, DeVries & Burke [1957]

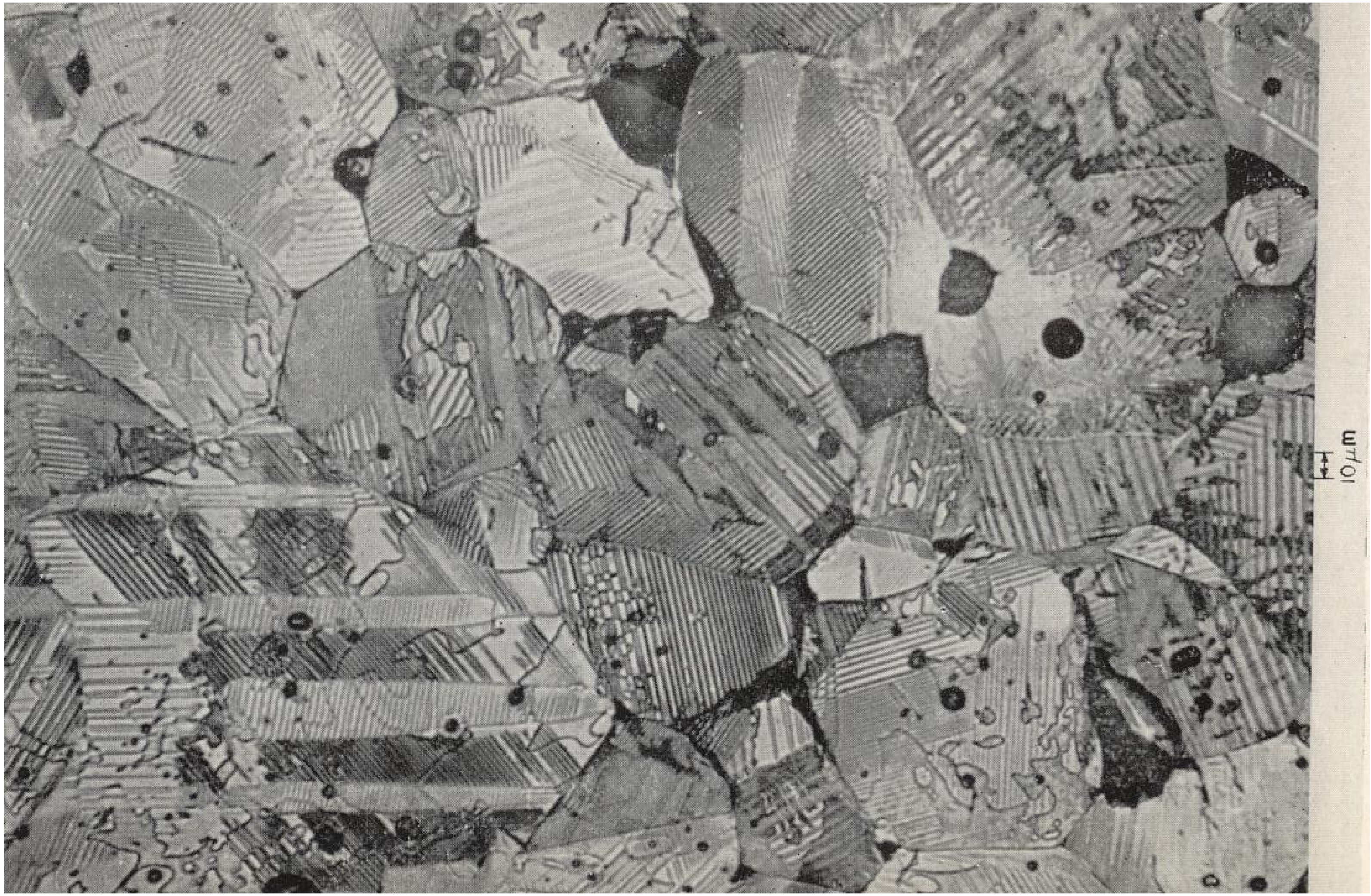

piezoceramics

- switching mechanisms

$|\mathrm{E}| > \mathrm{E_c}$: ferroelectricity

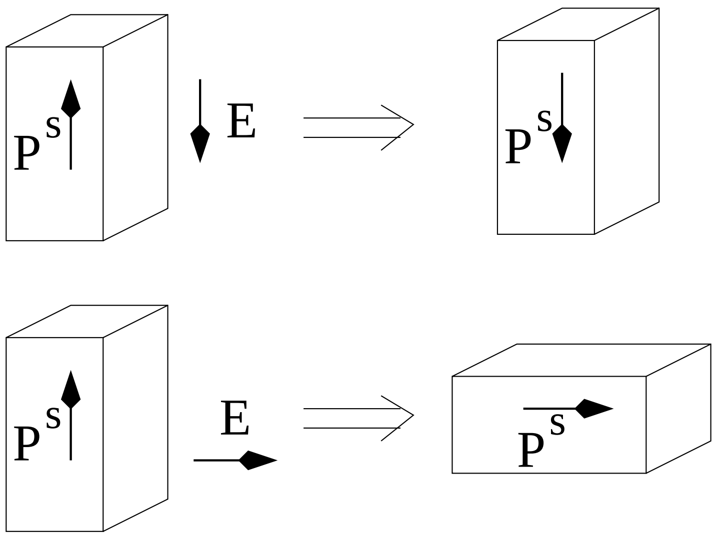

$|\sigma| > \sigma_\mathrm{c}$: ferroelasticity

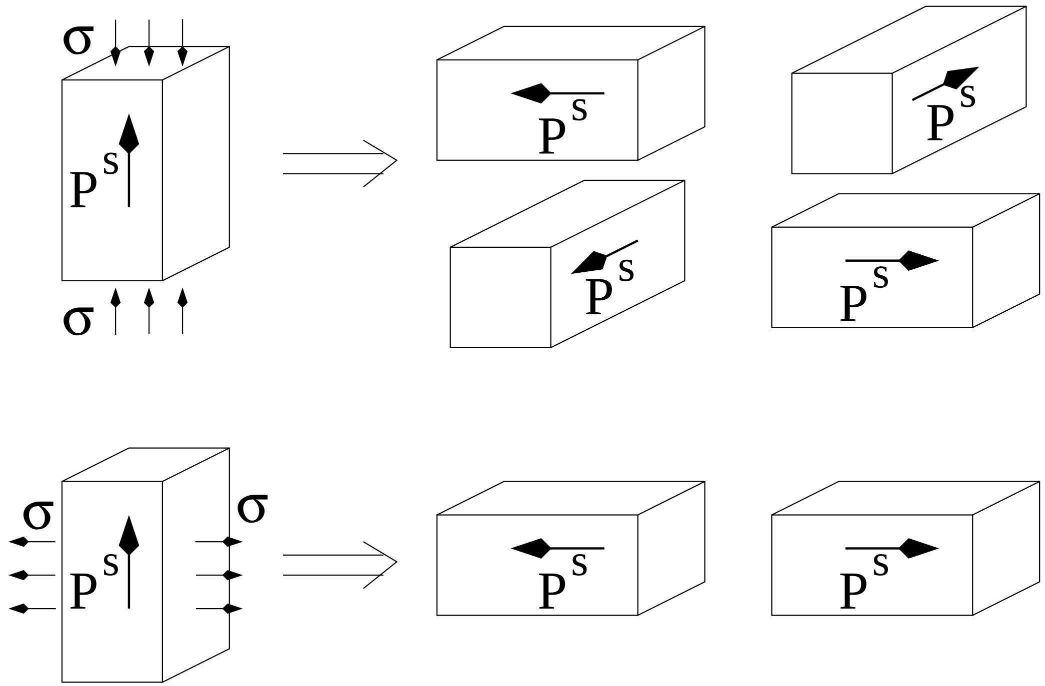

$\longrightarrow$ limits of linear behavior: large signal regime

experiments

setup: ZHOU [2003]

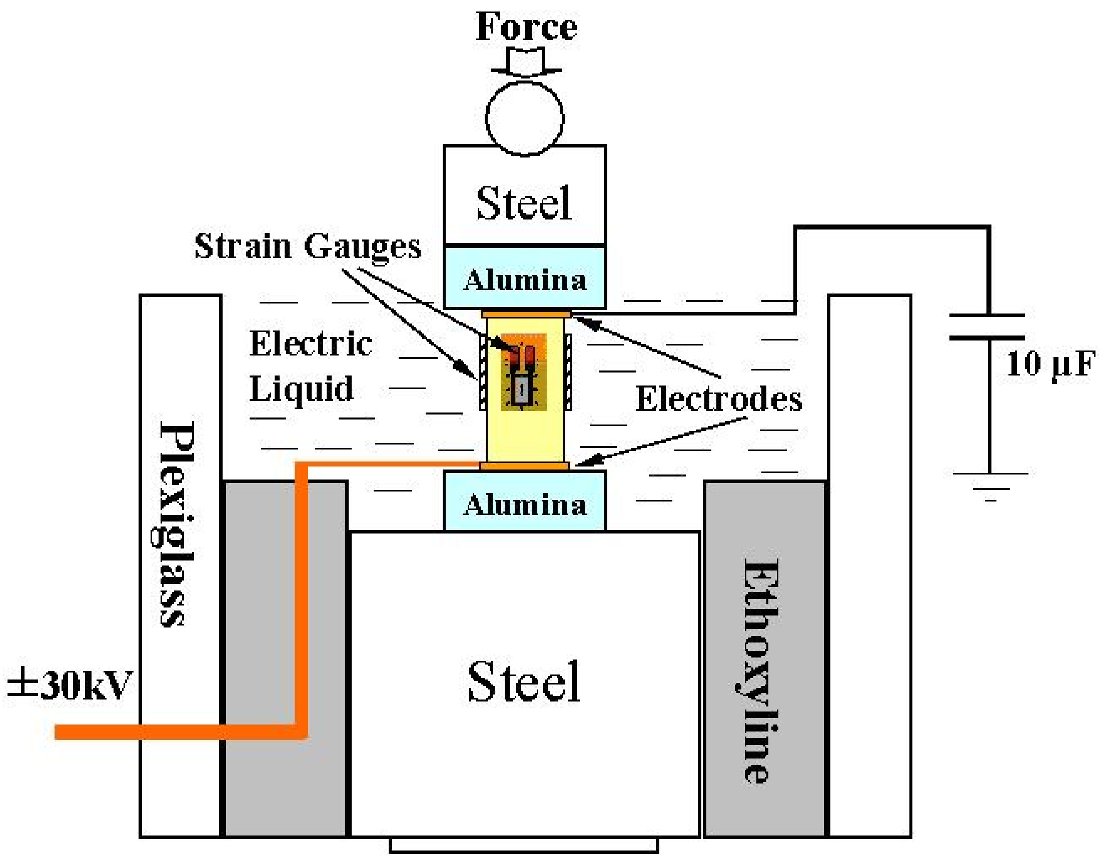

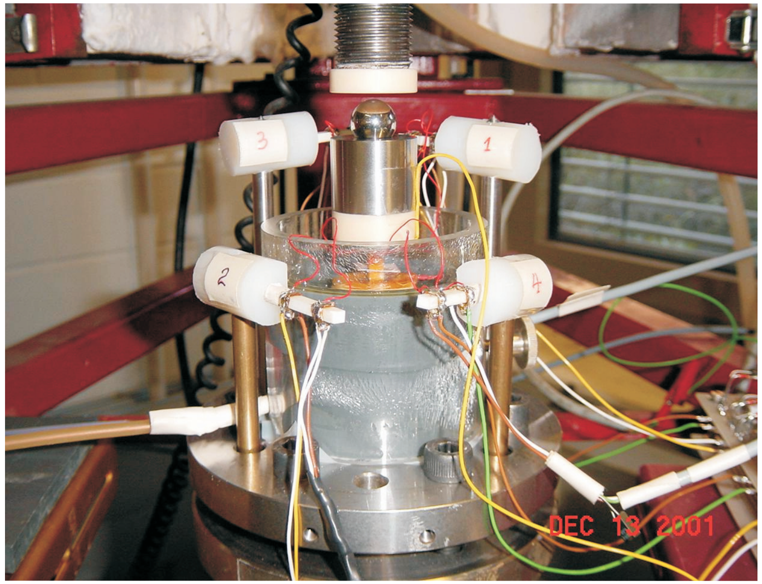

- material: soft-PZT PIC 151

  PI Ceramic, Lederhose (Thüringen)

hysteresis properties of ferroelectric ceramics

dielectric hysteresis

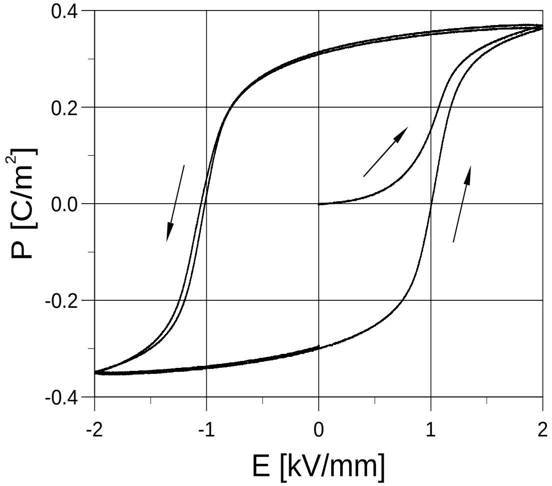

butterfly hysteresis

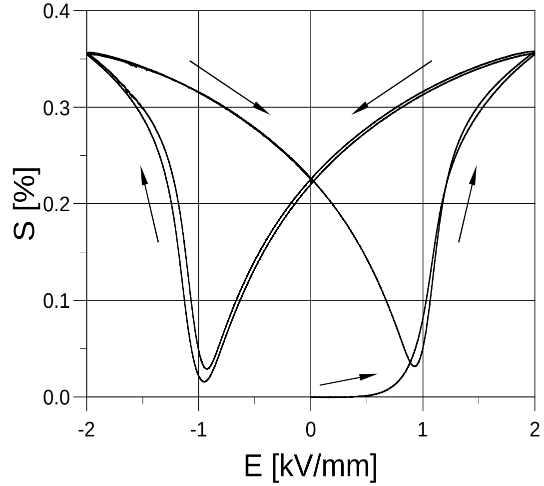

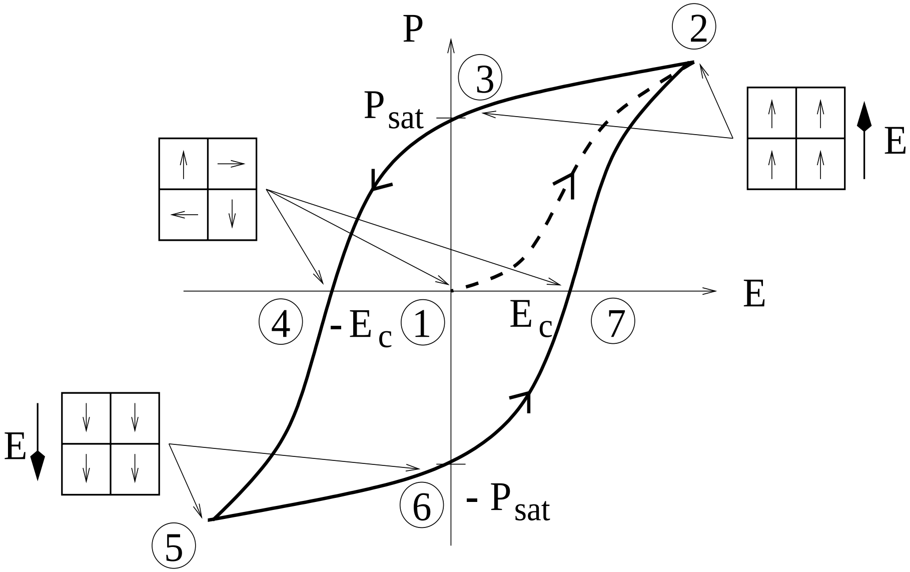

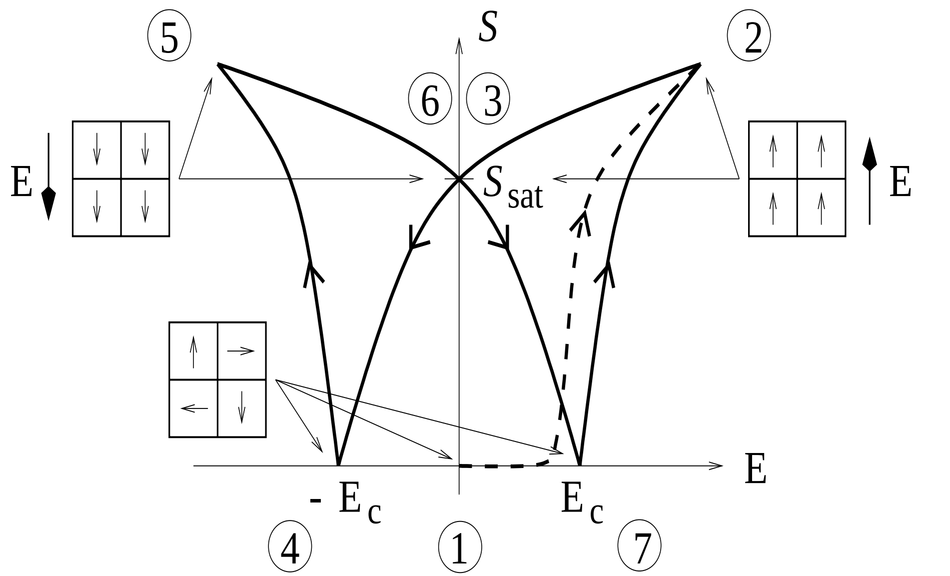

hysteresis properties of ferroelectric ceramics

ferroelastic hysteresis

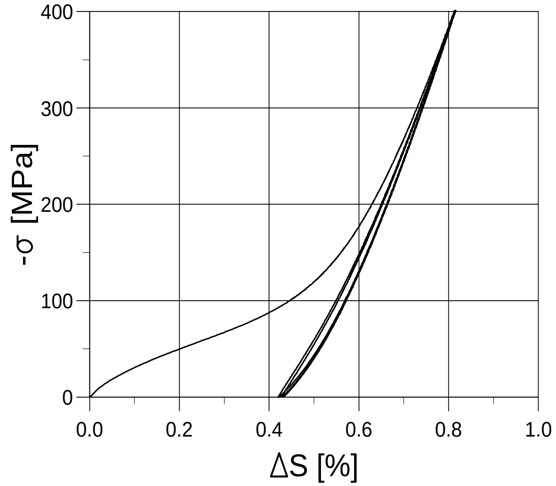

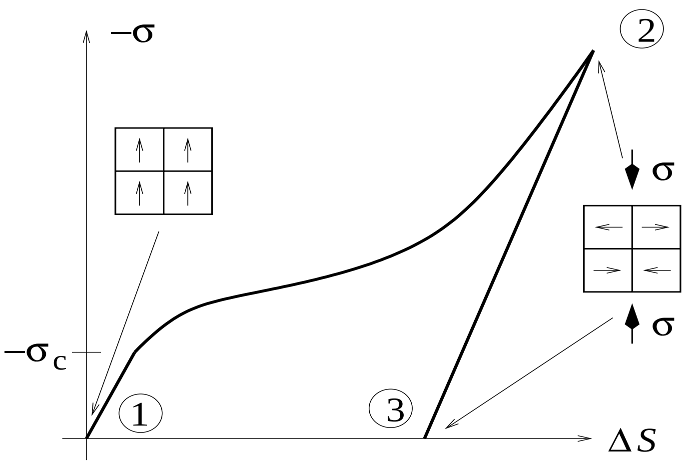

mechanical depolarization

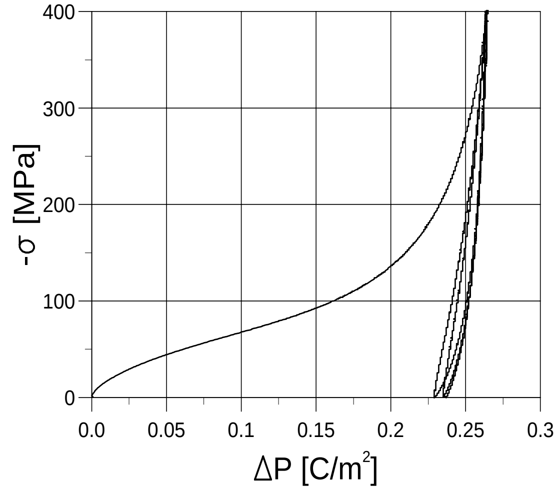

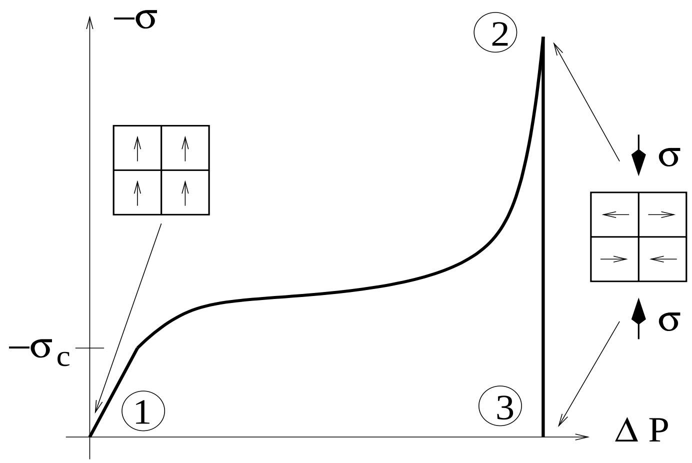

- field depended coercive stress, time and temperature effects, ...

electro-mechanical switching criterion

- uniaxial compression: equal critical stresses for unpoled and poled states
- proportional loading paths

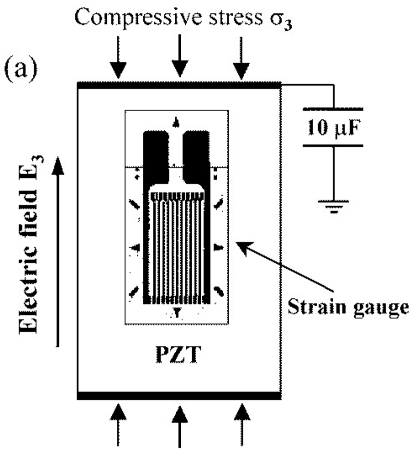

T_{33} *vs.* E_3

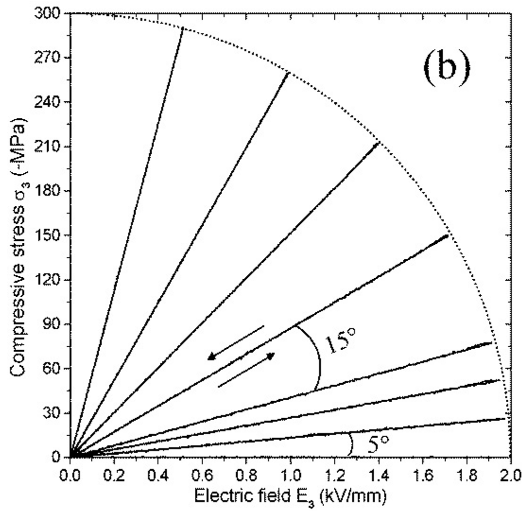

- D_3 *vs.* E_3 $\qquad$ S_{33} *vs.* E_3

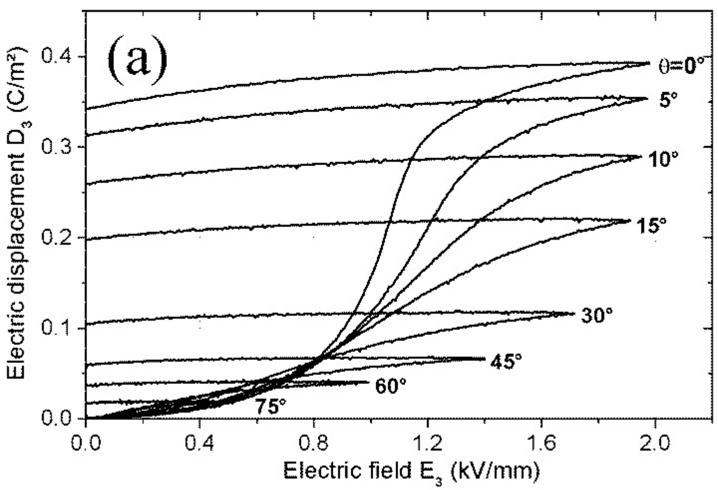

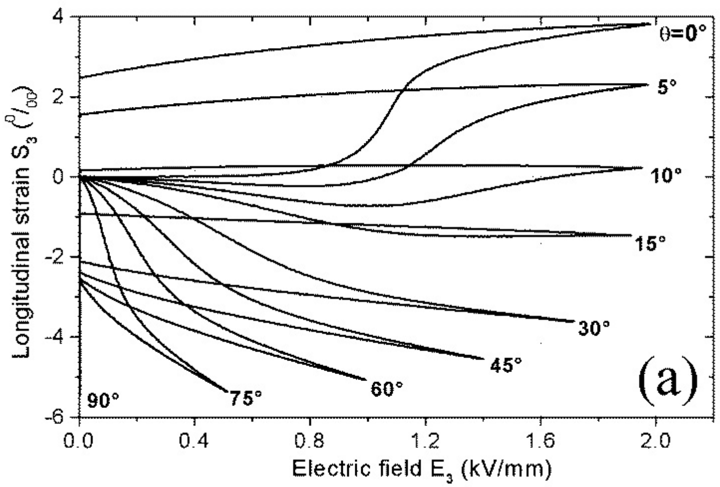

electro-mechanical switching criterion

- evaluation by offset method: (a) D_3 *vs.* E_3, (b) S_{33} *vs.* E_3

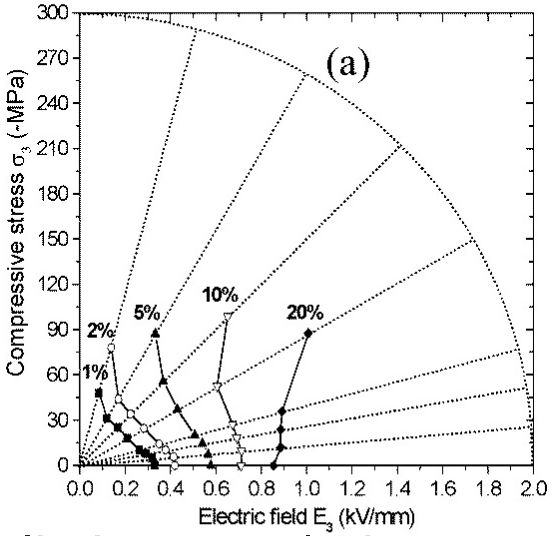

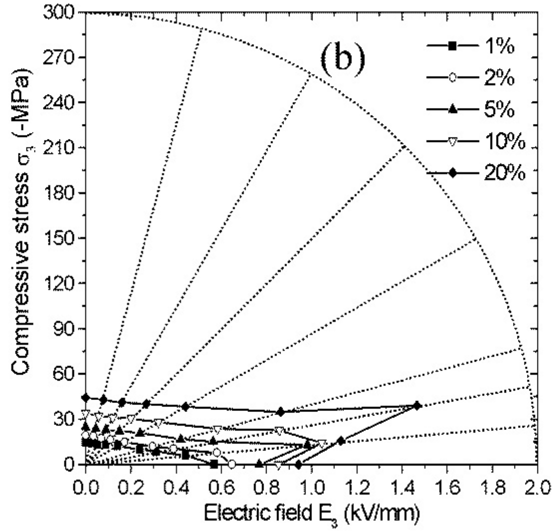

- preliminary analysis

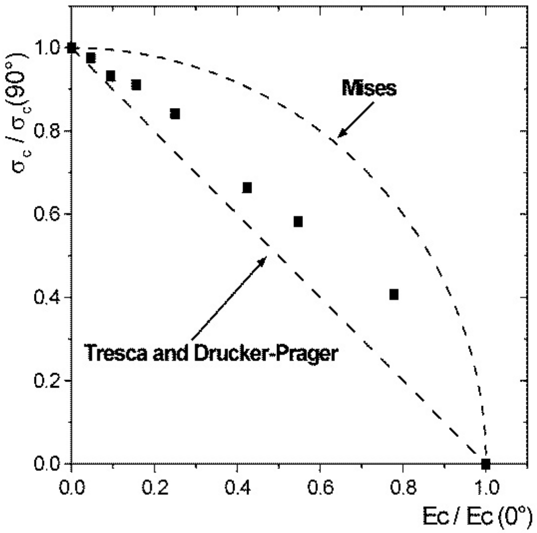

- von Mises

$$\left(\frac{T_{33}}{\sigma^{\mathrm{c}}}\right)^2 + \left(\frac{\mathrm{E}_3}{\mathrm{E}^{\mathrm{c}}}\right)^2 = 1$$

- Tresca/Drucker-Prager

$$\left|\frac{T_{33}}{\sigma^{\mathrm{c}}} + \frac{|\mathrm{E}_3|}{\mathrm{E}^{\mathrm{c}}}\right| = 1$$

structure of continuum theory

($\longrightarrow$ *see presentation by Volkmar Mehling*)

- universal balance laws
  - dynamics: balance of linear momentum

    $$\rho\,\ddot{\vec{\mathrm{u}}} = \mathsf{div}\,\boldsymbol{T} + \rho\,\vec{\mathrm{k}}$$

  - quasi-electrostatics: Gaussian law

    $$\mathsf{div}\,(\epsilon_0 \vec{\mathrm{E}} + \vec{\mathrm{P}}) = q^{\mathrm{ext}}$$

- macroscopic constitutive model, geometrically linear

$$\left.\begin{array}{c}\boldsymbol{T}\\ \vec{\mathrm{P}}\end{array}\right\} \quad \longleftrightarrow \quad \left\{\begin{array}{l}\boldsymbol{S} = \frac{1}{2}\Big(\mathsf{grad}\vec{\mathrm{u}} + (\mathsf{grad}\vec{\mathrm{u}})^T\Big)\\ \vec{\mathrm{E}} = -\mathsf{grad}\varphi\end{array}\right.$$

  - micromechanics
  - phenomenological methods

micromechanics

volume element: KAMLAH & MCMEEKING [2002]

- plane strain

  10×10 ferroelectric grains (HUBER *et al.* [1999])

  $\mathrm{E}^{\mathrm{av}} = -\varphi/h$

  $\mathrm{D}^{\mathrm{av}} = -Q/h$

  $S^{\mathrm{av}} = u/h$

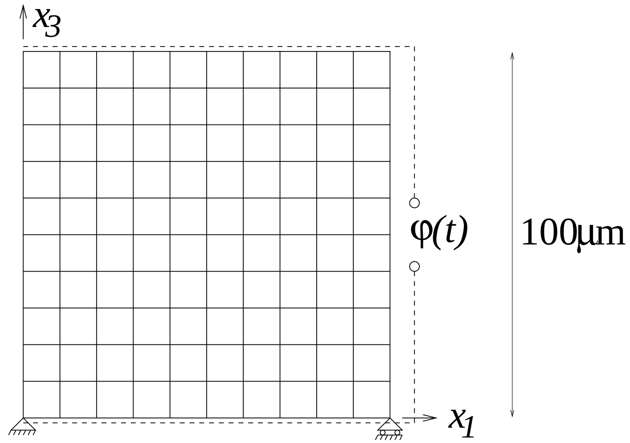

- macroscopic response of polycrystal during poling

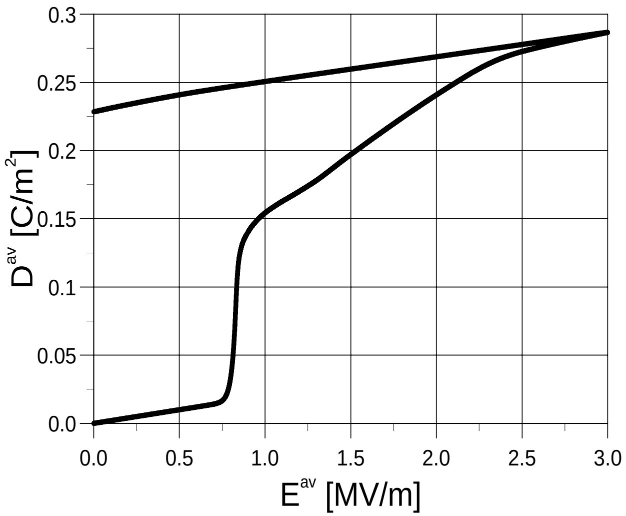

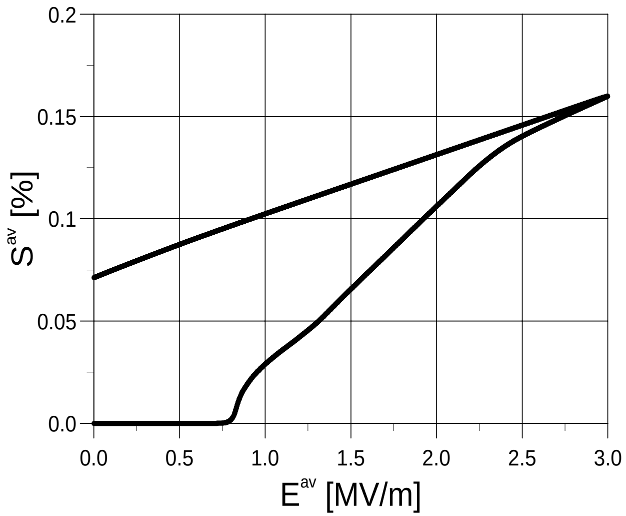

$\longrightarrow$ averaging over orientation distribution, grain to grain interaction

generally accepted structure of constitutive models

Cocks & McMeeking [1999], Kamlah & Jiang [1999], ...

- additive decomposition into reversible and irreversible parts

$$\boldsymbol{S} = \boldsymbol{S}^{\mathrm{r}} + \hat{\boldsymbol{S}}^{\mathrm{i}}(q^1, \ldots, q^n)$$

$$\vec{\mathrm{P}} = \vec{\mathrm{P}}^{\mathrm{r}} + \hat{\vec{\mathrm{P}}}^{\mathrm{i}}(q^1, \ldots, q^n)$$

$q^1, \ldots, q^n$: microstructural variables

- representation of reversible behavior

$$\boldsymbol{S}^{\mathrm{r}} = \mathbb{C}^{-1} : \boldsymbol{T} + \hat{\mathbf{d}}^T \cdot \vec{\mathrm{E}}$$

$$\vec{\mathrm{P}}^{\mathrm{r}} = \hat{\mathbf{d}} : \boldsymbol{T} + \boldsymbol{\kappa} \cdot \vec{\mathrm{E}}$$

- history dependent anisotropy, $\mathrm{e}_i = (\vec{\mathrm{e}}^{\mathrm{P}^{\mathrm{i}}})_i$

$$\hat{\mathrm{d}}_{kij}(q^1, \ldots, q^n) = \frac{\left\|\vec{\mathrm{P}}^{\mathrm{i}}\right\|}{\mathrm{P}^{\mathrm{sat}}} \Big\{ \mathrm{d}_{33}\, \mathrm{e}_i\, \mathrm{e}_j\, \mathrm{e}_k + \mathrm{d}_{31}\, (\delta_{ij} - \mathrm{e}_i\, \mathrm{e}_j)\, \mathrm{e}_k + \mathrm{d}_{15}\, \frac{1}{2} \Big[(\delta_{ki} - \mathrm{e}_k\, \mathrm{e}_i)\, \mathrm{e}_j + (\delta_{kj} - \mathrm{e}_k\, \mathrm{e}_j)\, \mathrm{e}_i \Big] \Big\}$$

$\longrightarrow$ thermodynamical consistency *(see presentation by Volkmar Mehling)*

microscopically motivated constitutive model

uniaxial formulation

- 45° cones about axis of loading

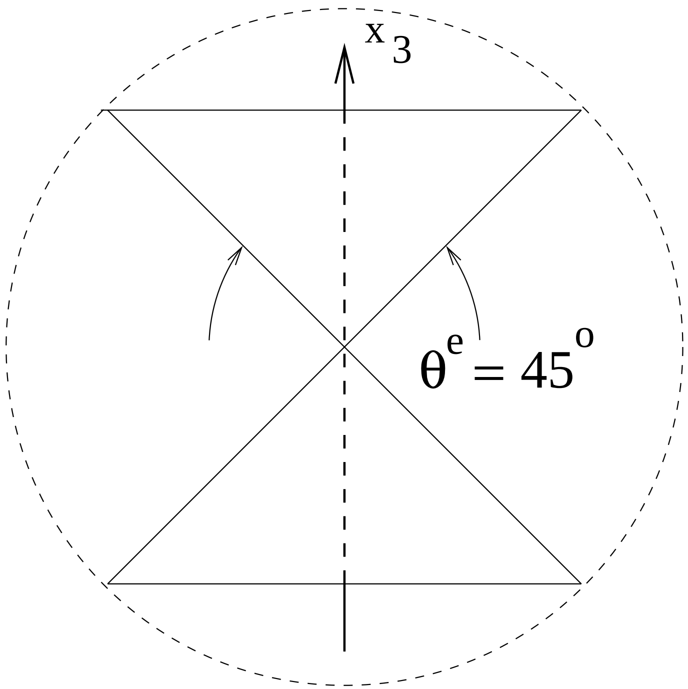

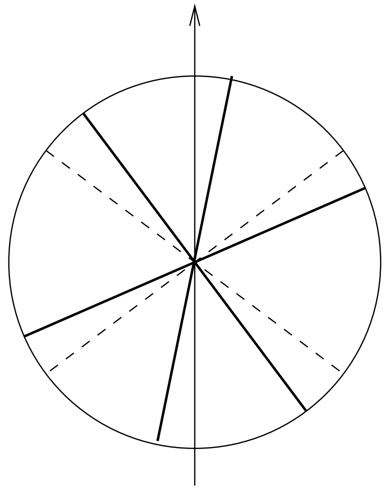

$q^1 = \beta \; \in \; [0,1]$:

fraction of aligned c-axes

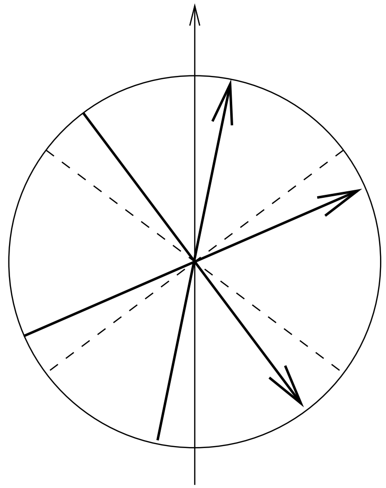

$q^2 = \gamma \; \in \; [-1,1]$:

relative irreversible polarization

interpretation as orientation distribution function (Kamlah & Wang [2003])

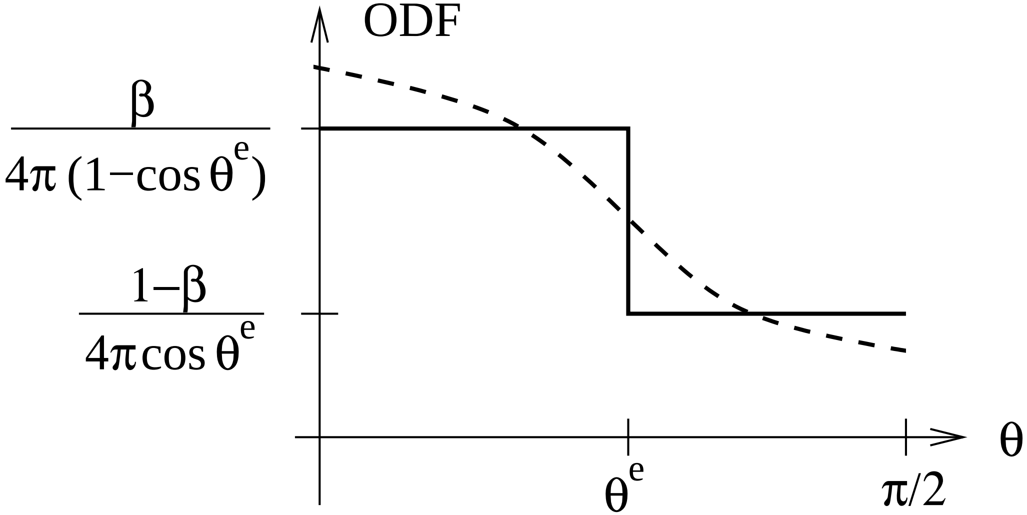

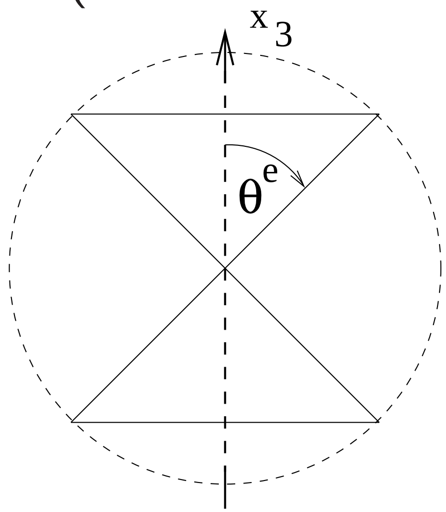

- integration: irreversible strain

$$S^{\mathrm{i}}_{33} \;=\; \tfrac{3}{2}(\beta - \tfrac{1}{3})S^{\mathrm{sat}}\,, \qquad -\tfrac{1}{2}S^{\mathrm{sat}} \;\leq\; S^{\mathrm{i}}_{33} = \tfrac{3}{2}(\beta - \tfrac{1}{3})S^{\mathrm{sat}} \;\leq\; S^{\mathrm{sat}}$$

- integration: maximum irreversible polarization

$$\mathrm{P}^{\mathrm{i}}_{3} = \gamma \mathrm{P}^{\mathrm{sat}}\,, \qquad \mathrm{P}^{\mathrm{i}}_{3} \;\leq\; \frac{3\,\beta + 2}{5}\,\mathrm{P}^{\mathrm{sat}}$$

$\longrightarrow$ Gibbs energy $g(\beta, \gamma)$, switching function $f(\phi^{\beta}, \phi^{\gamma})$: evolution equations

(see presentation by Volkmar Mehling)

microscopically motivated constitutive model

dielectric hysteresis

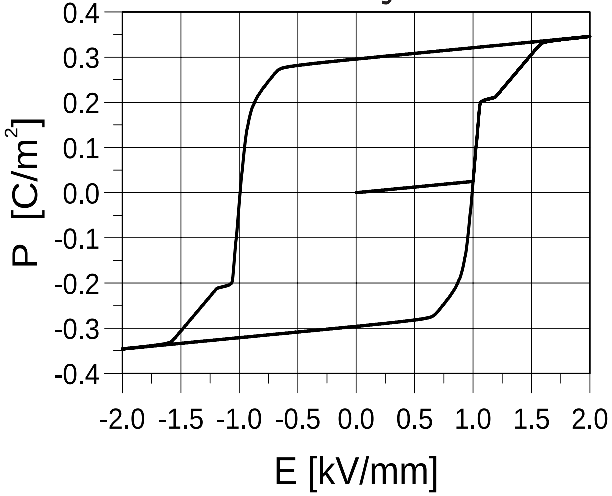

butterfly hysteresis

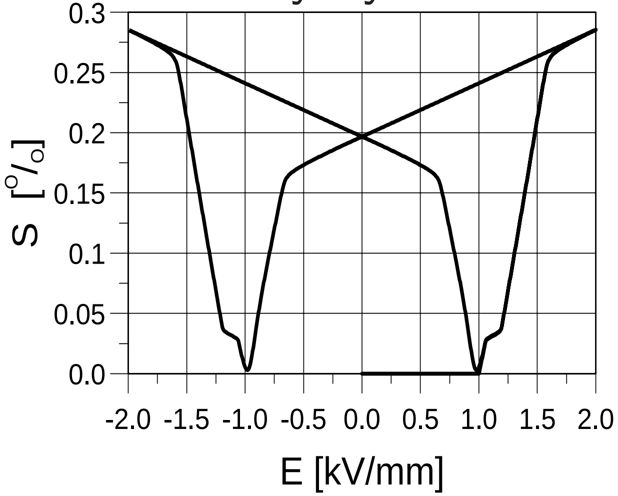

ferroelastic hysteresis

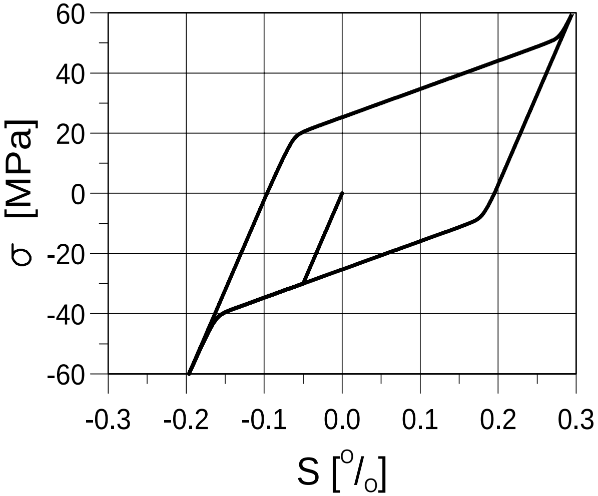

mechanical depolarization

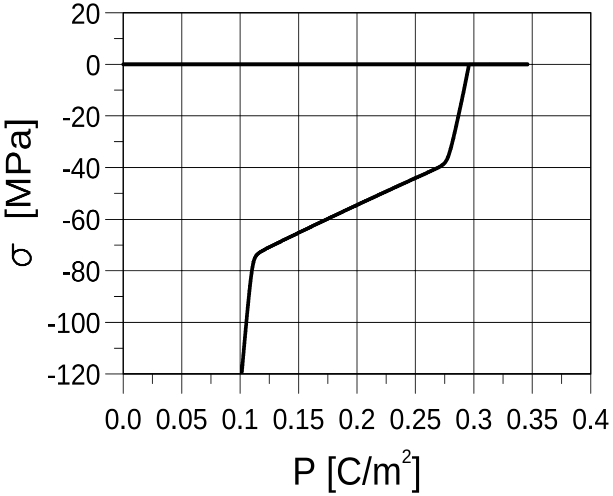

three-dimensional domain state

- simplified representation

  $\vec{\mathrm{e}}^{\beta}$: history dependent axis of transversely isotropic ODF

- integration: irreversible strain

$$\boldsymbol{S}^{\mathrm{i}} = \frac{3}{2} S^{\mathrm{sat}} \frac{\beta - \beta^{\mathrm{ref}}}{1 - \beta^{\mathrm{ref}}} \left(\vec{\mathrm{e}}^{\beta} \otimes \vec{\mathrm{e}}^{\beta} - \tfrac{1}{3} \boldsymbol{I} \right)$$

  $\longrightarrow$ uniaxial, volume preserving

- irreversible polarization

$$\vec{\mathrm{P}}^{\mathrm{i}} = \gamma \, \vec{\mathrm{e}}^{\gamma}$$

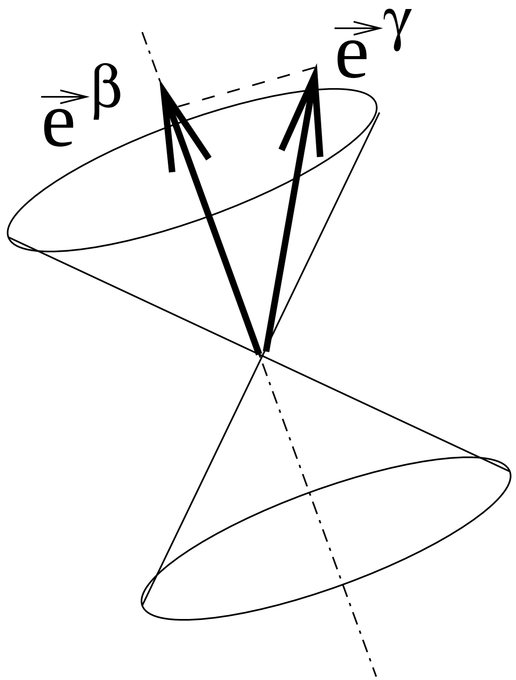

$\longrightarrow$ two additional vectorial internal variables $\vec{\mathrm{e}}^{\beta}$, $\vec{\mathrm{e}}^{\gamma}$

microscopically motivated constitutive model

- non-proportional poling (Huber & Fleck [2001])

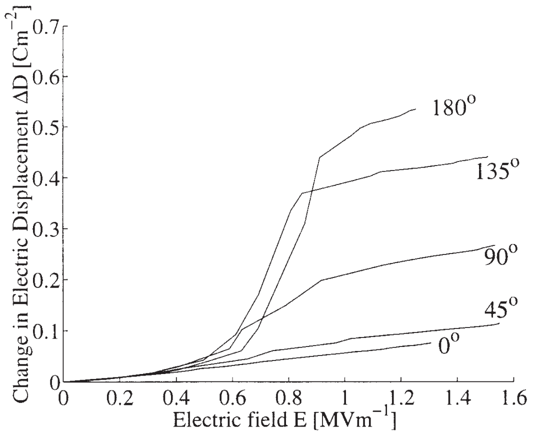

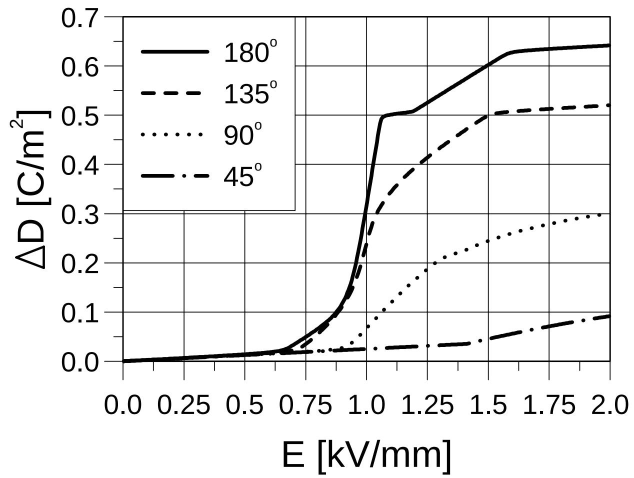

- cyclic shearing after full poling

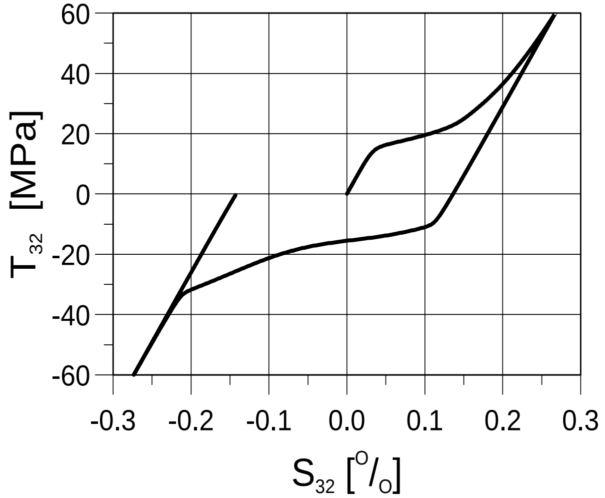

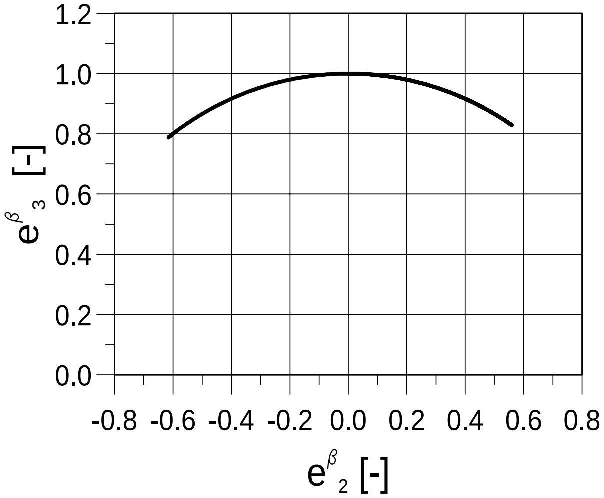

→ finite element implementation: current project

simple phenomenological constitutive model

formulation based on loading conditions: Kamlah & Böhle [2001]

- two contributions to the irreversible strain

$$\boldsymbol{S}^{\mathrm{i}} = \boldsymbol{S}^{\mathrm{p}} + \boldsymbol{S}^{\mathrm{f}}$$

with

$$\boldsymbol{S}^{\mathrm{p}} = \frac{3}{2}\, S_{\mathrm{sat}} \frac{\|\vec{\mathrm{P}}^{\mathrm{i}}\|}{\mathrm{P}_{\mathrm{sat}}} \left(\vec{\mathrm{e}}_{\mathrm{P}^{\mathrm{i}}} \otimes \vec{\mathrm{e}}_{\mathrm{P}^{\mathrm{i}}} - \frac{1}{3}\boldsymbol{I} \right)$$

- onset of switching

$$\underline{f^{\mathrm{p}} = \|\vec{\mathrm{E}} - c^{\mathrm{p}}\, \vec{\mathrm{P}}^{\mathrm{i}}\| - \mathrm{E}_{\mathrm{c}} = 0}$$

$$f^{\mathrm{f}} = \sqrt{\frac{3}{2}}\, \|(\boldsymbol{T} - c^{\mathrm{f}}\, \boldsymbol{S}^{\mathrm{f}})^{D}\| - \hat{\sigma}_{\mathrm{c}} = 0$$

- fully switched domain structure

$$\underline{h^{\mathrm{p}} = \|\vec{\mathrm{P}}^{\mathrm{i}}\| - \hat{\mathrm{P}}_{\mathrm{sat}} = 0}$$

$$h^{\mathrm{f}} = \sqrt{\frac{2}{3}}\, \|\boldsymbol{S}^{\mathrm{f}}\| - \left(S_{\mathrm{sat}} - \sqrt{\frac{2}{3}}\, \|\boldsymbol{S}^{\mathrm{p}}\|\right) = 0$$

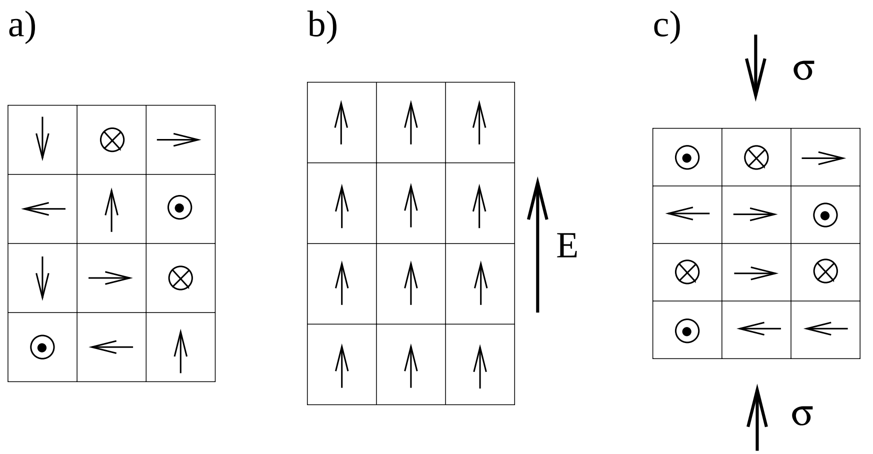

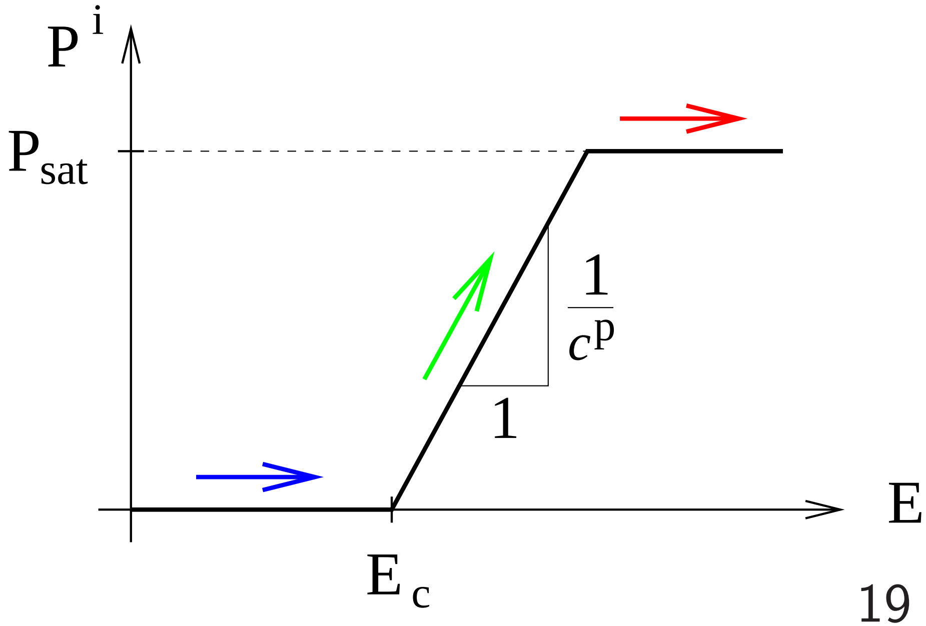

simple phenomenological constitutive model

representation of standard hystereses

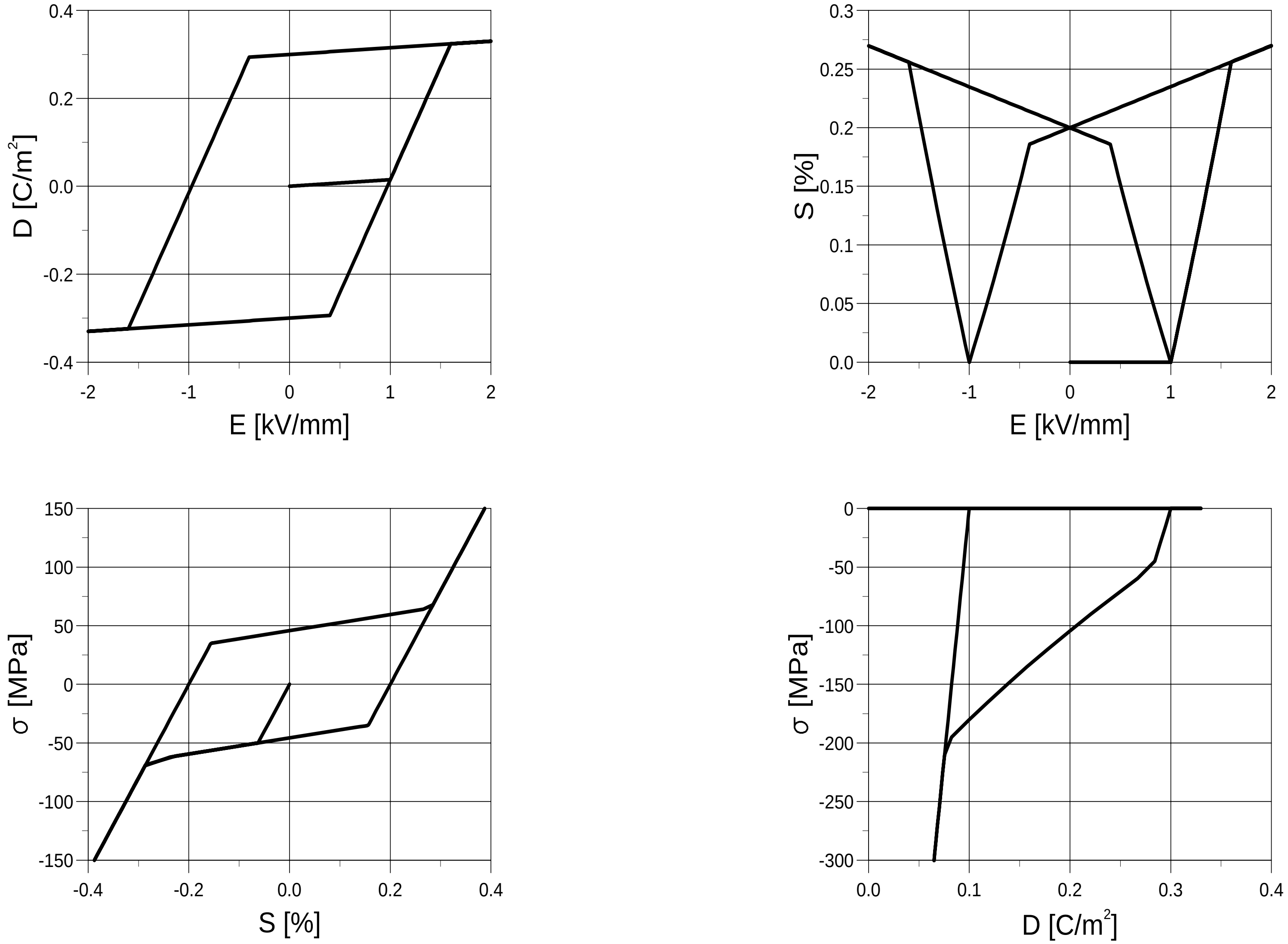

finite element implementation

radial-return-algorithm: LASKEWITZ & KAMLAH [2005]

- last equilibrium state: $\vec{\mathrm{E}}_n$, $\vec{\mathrm{P}}^{\mathrm{i}}_n$, $(\boldsymbol{S}_n, \boldsymbol{S}^{\mathrm{f}}_n)$
- Newton iteration

  given: $\vec{\mathrm{E}}_{n1}$, $(\boldsymbol{S}_{n1})$

  unknown: $\vec{\mathrm{P}}^{\mathrm{i}}_{n1}$, $(\boldsymbol{S}^{\mathrm{f}}_{n1})$

- electric switching criterion

  $$\frac{f^{\mathrm{p}}}{c^{\mathrm{p}}} = \left\| \frac{\vec{\mathrm{E}}_{n1}}{c^{\mathrm{p}}} - \vec{\mathrm{P}}^{\mathrm{i}}_n \right\| - \frac{\mathrm{E}^{\mathrm{c}}}{c^{\mathrm{p}}} > 0 \rightarrow \Delta\vec{\mathrm{P}}^{\mathrm{i}}_f$$

- electric saturation criterion

  $$h^{\mathrm{p}} = \left\| \vec{\mathrm{P}}^{\mathrm{i}}_n + \Delta\vec{\mathrm{P}}^{\mathrm{i}}_f \right\| - \mathrm{P}_{\mathrm{sat}} > 0 \rightarrow \Delta\vec{\mathrm{P}}^{\mathrm{i}}_h$$

- update of internal variable

  $$\vec{\mathrm{P}}^{\mathrm{i}}_{n1} = \vec{\mathrm{P}}^{\mathrm{i}}_n + \Delta\vec{\mathrm{P}}^{\mathrm{i}}_f + \Delta\vec{\mathrm{P}}^{\mathrm{i}}_h$$

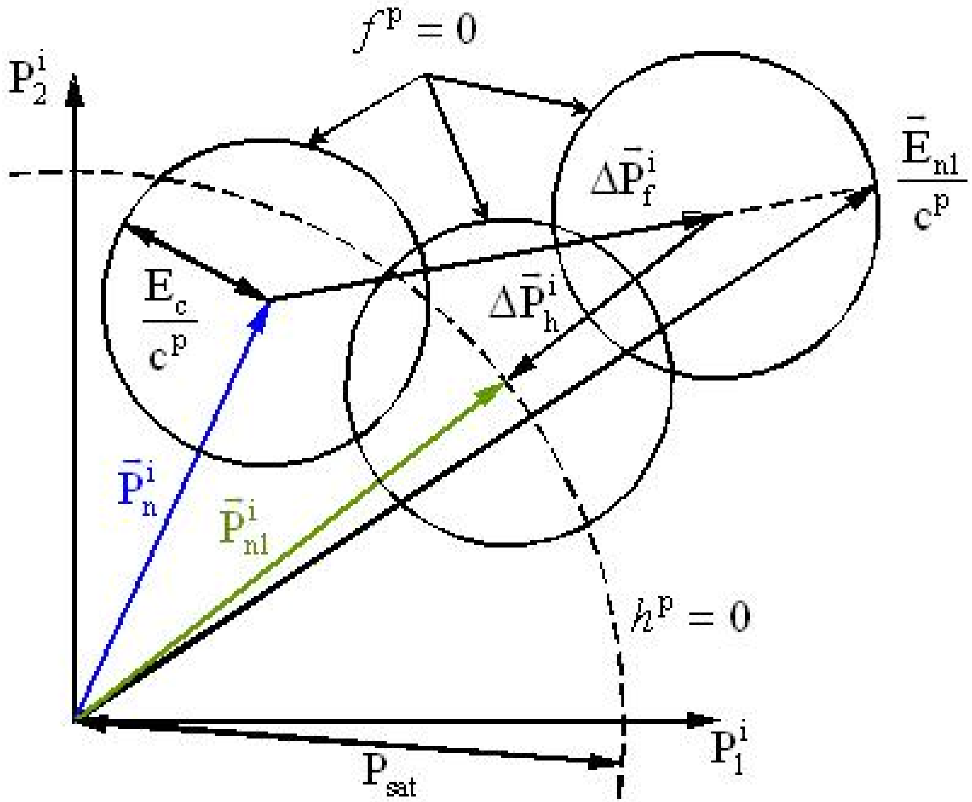

finite element analysis

simplified model: poling stresses in stack actuator

- symmetries

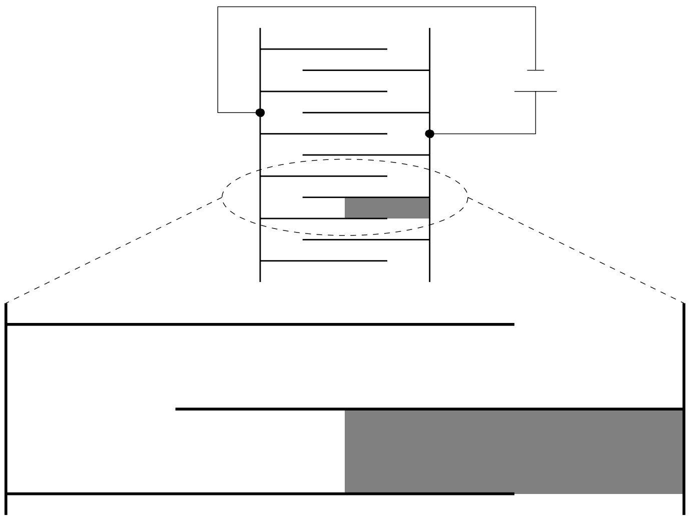

- FE model, plane strain

$\varphi = 0$, all nodes same u_2, $\int T_{22}\, dx_1 = 0$

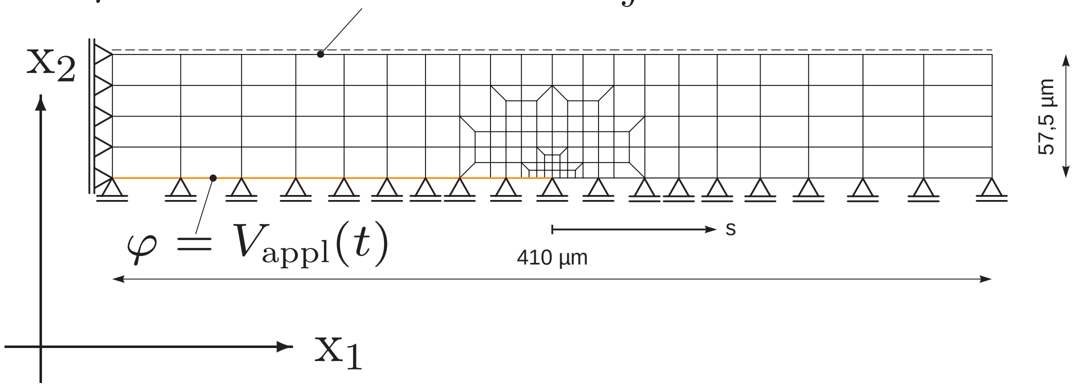

- irreversible polarization after poling

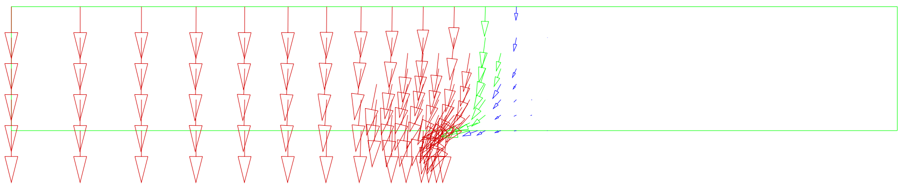

- residual stresses along lower edge

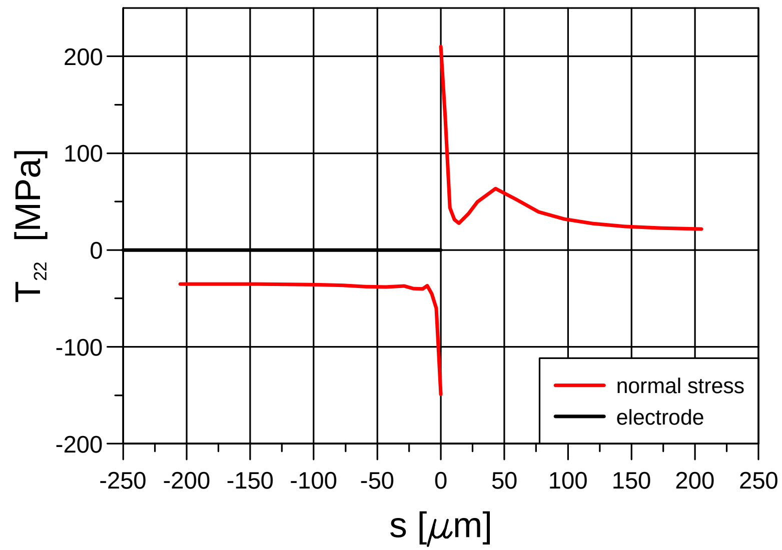

$\longrightarrow$ influence of hysteresis effects on poled state

finite element analysis

1-3 composite PZT-polymer (Univ. Halle)

- PZT: 5% . . . 65%

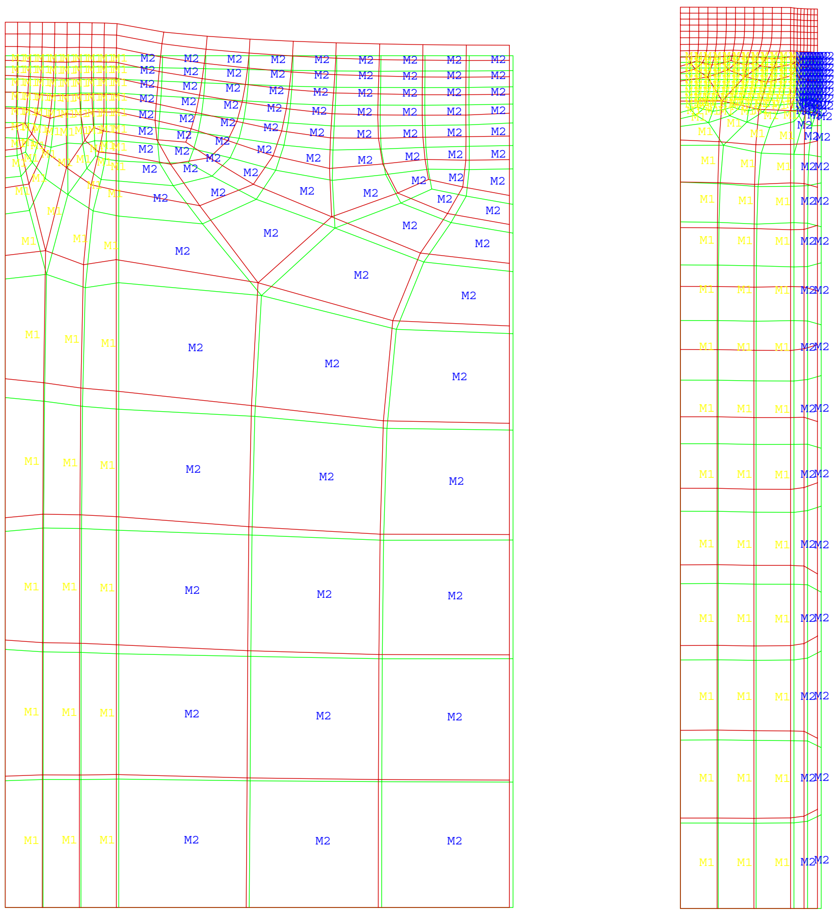

→ matrix: mechanical depolarization

poling cracks (Univ. Darmstadt)

- partly electroded specimens

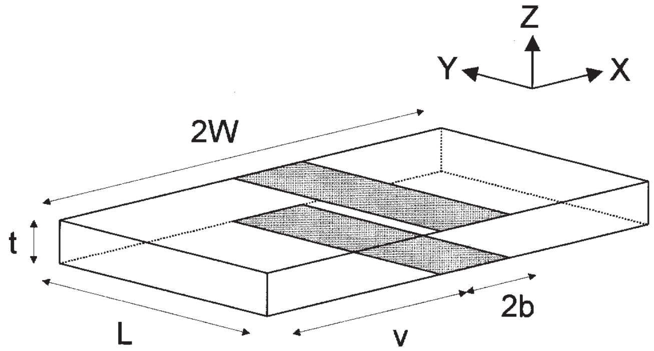

- $t = 0.5, 1.0, 2.0$ mm, $\mathrm{E_{nom}} = 2\,\mathrm{E^c}$

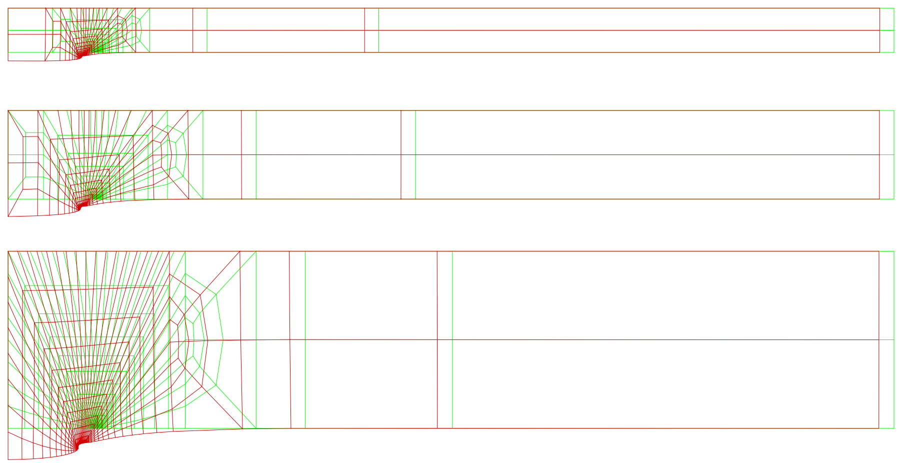

→ inhomogenous poling: stresses

summary

- ferroelectric piezoceramics
- response behavior

  hysteresis properties, electro-mechanical switching surface

$\longrightarrow$ strong non-linear coupling of irrev. polarization, irrev. strain, piezoelectricity, ...

- micromechanical volume element
- micromechanically motivated constitutive model

  internal variables for orientation distribution function

  three dimensional formulation

$\longrightarrow$ correct representation of tensorial properties

- finite element simulation of poling processes

  simple phenomenological constitutive law, finite element implementation

  stack actuator, 1-3 composite, poling cracks

$\longrightarrow$ spatial distribution of macroscopic electro-mechanical fields